Impurity Transport Experiments at the HSX Stellarator with Laser Blow-Off Injections

J.F. Castillo, B. Geiger, A. Bader, S.T.A Kumar,
K.M. Likin, D.T. Anderson

HSX Plasma Laboratory, Univ. of Wisconsin-Madison, USA

62nd Annual Meeting of the APS Division of Plasma Physics

November 9-13, 2020

 This work is supported by US DOE Grant DE-FG02-93ER5422

Impurity Transport Experiments at HSX

Motivation to study impurity transport:

- Impurities dilute fuel and radiate away energy from the plasma
  - Too much He ‘ash’ in core
  - Wall-sourced impurities accumulate
- Predict and control impurity accumulation
  - Impurity transport is a serious constraint and needs to be better understood in 3-D fusion devices

Helically Symmetric eXperiment

- Optimized Stellarator – **Q**uasi-**H**elical **S**ymmetry
- 4 field periods, 12 modular coils per period
- 48 auxiliary coils for configuration flexibility

‘Typical’ plasma discharge QHS, 1 Tesla

- QHS, 1 Tesla, 50 kW injected power
- Absorbed ECH power is ≈ 11.3 kW, deposited on-axis

HSX Cutaway

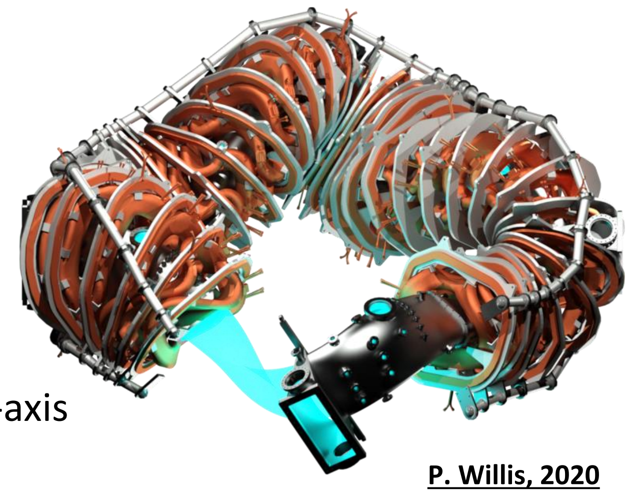

P. Willis, 2020

Goals of this study:

- Quantify impurity transport in the HSX stellarator
- Compare these results to neoclassical calculations to determine whether transport is anomalous

Electron Temperature

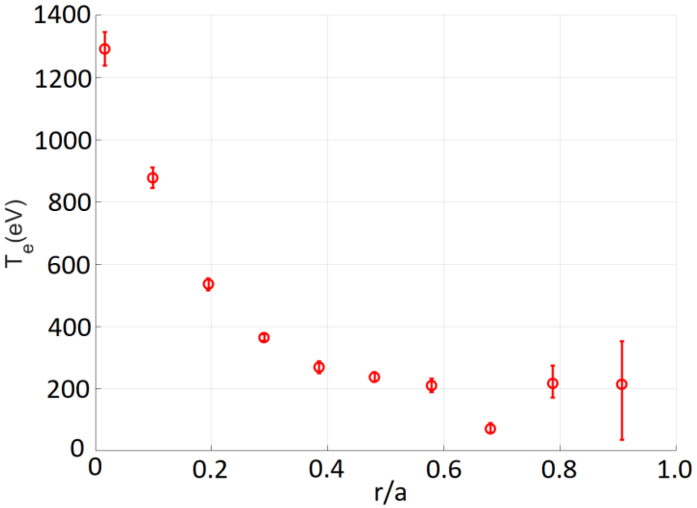

Electron Density

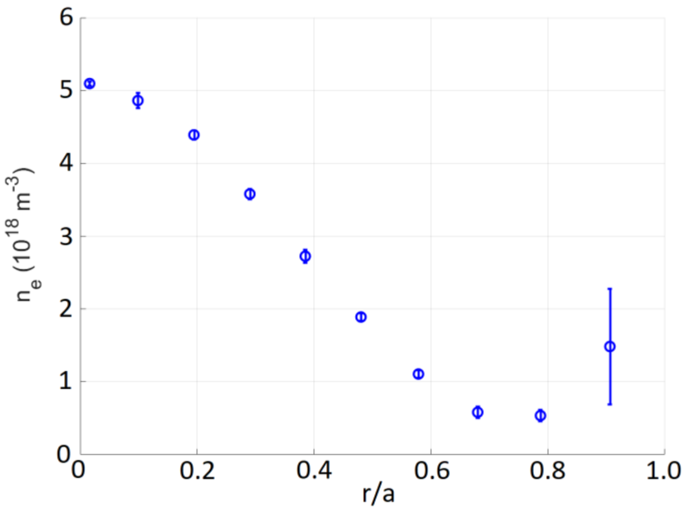

Impurity Injection by Laser Blow-Off (LBO)

Impurity injection by laser blow-off (LBO)

- A laser illuminates a thin film of tracer material on a target area
- Resulting neutrals ballistically enter plasma and emit radiation
- Quantity of neutrals is controllable
- Photodiode detectors measure impurity radiation

HSX Aerial View

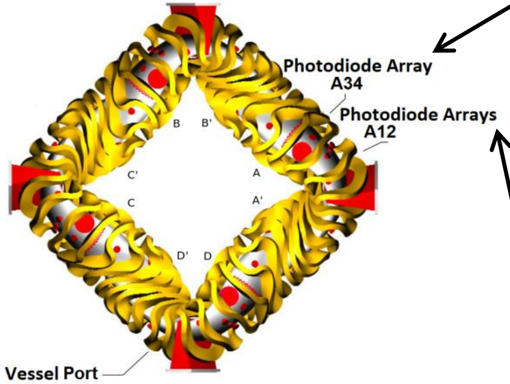

Lines-of-Sight for Photodiode A34

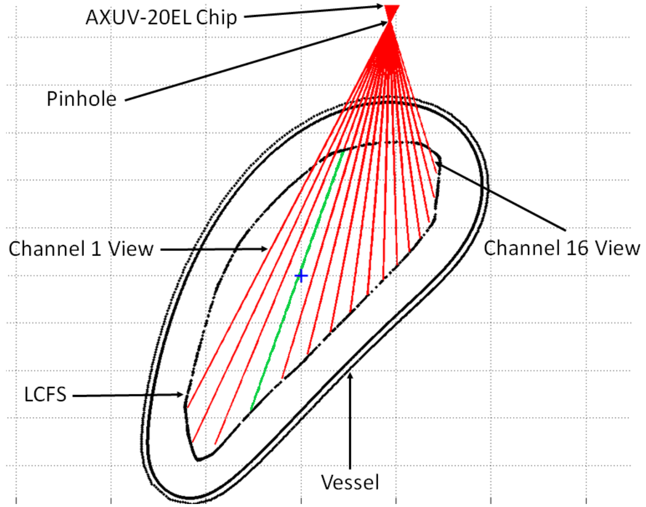

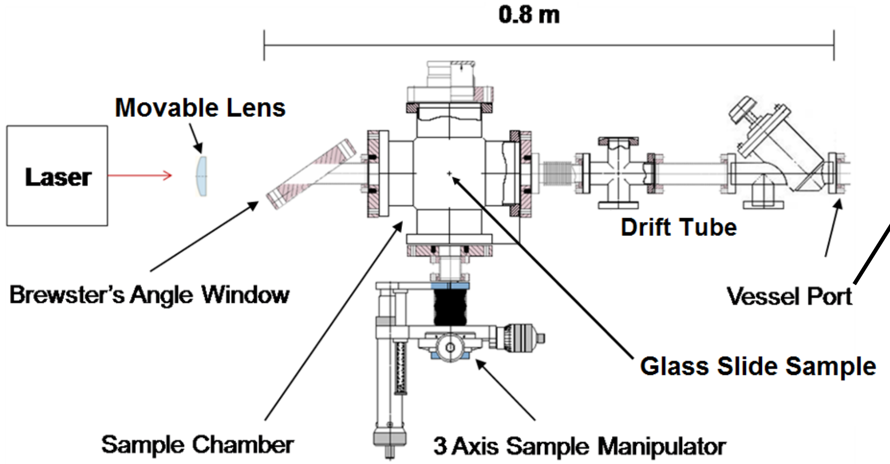

Schematic of HSX LBO System

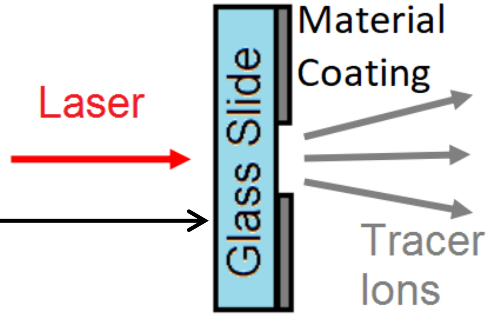

Laser Blow-Off Process

Lines-of-Sight for Photodiode A12M

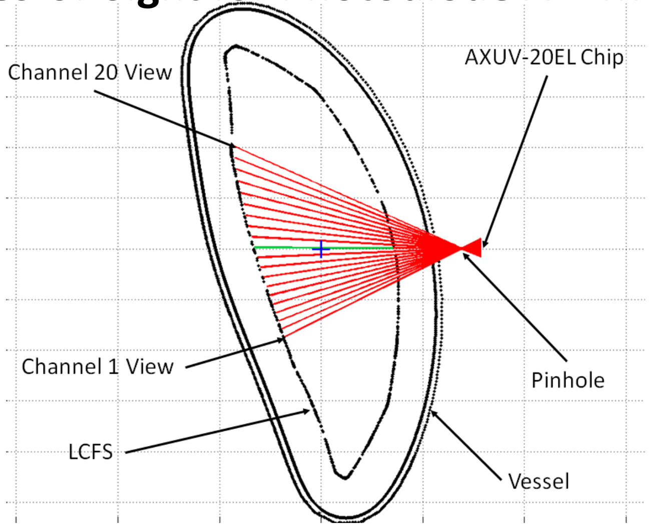

Good Signal to Noise Measurement Without Strong Density Perturbation

'Typical' QHS plasma discharge

- Impurity injections are performed with 2 µm aluminum layer over a 10 nm chromium layer
- Aluminum neutrals penetrate into plasma before ionizing
- Photodiode arrays measure the total radiation signal
- Signals provide line-integrated measurements of local emissivity
- Channel 4 of array A34 and channel 11 of A12 m are closest to center of core

Line-averaged Electron Density

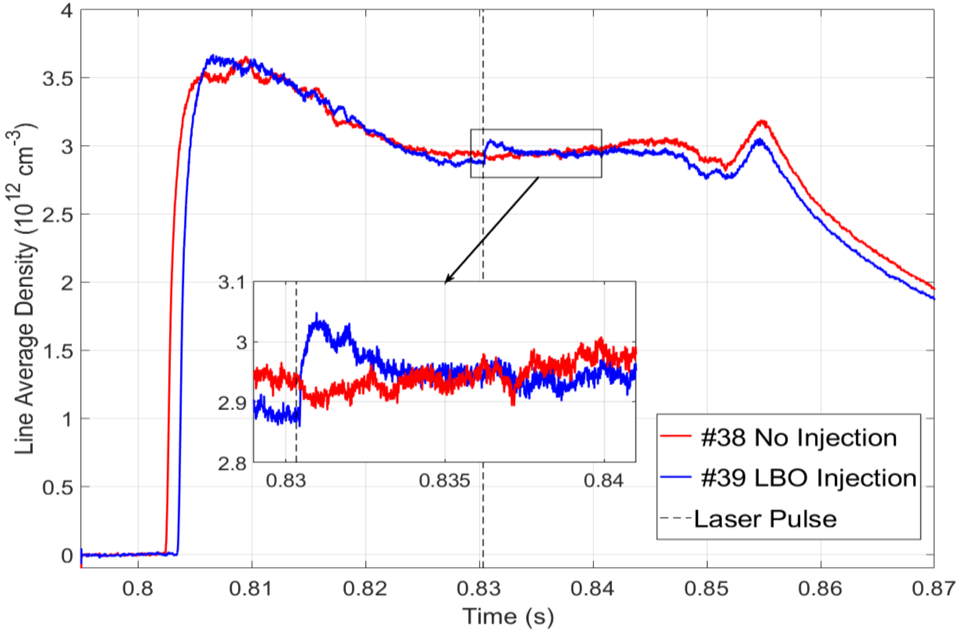

A12M 'Core' Channel 11

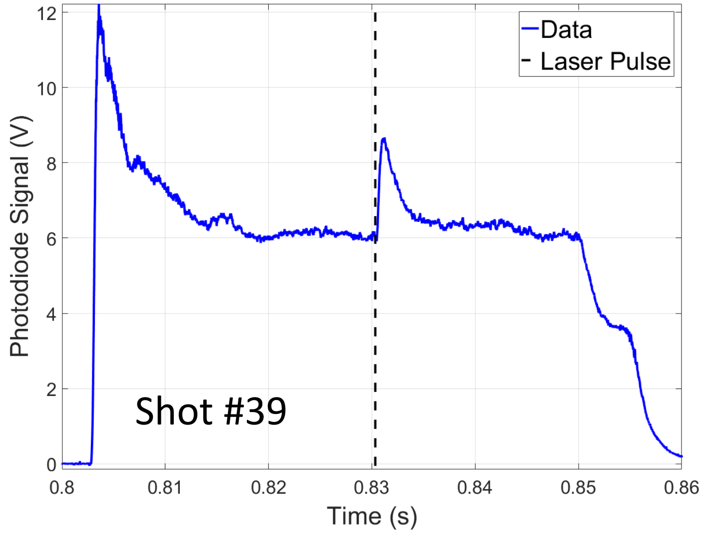

A34 'Core' Channel 4

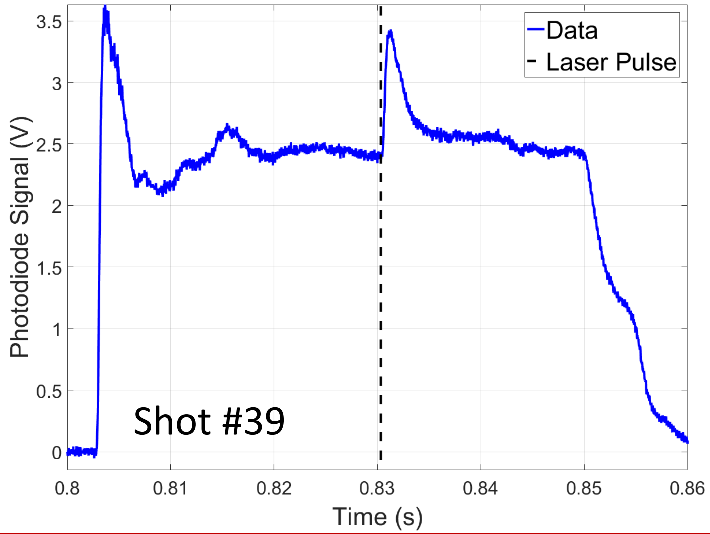

Simulating Experimental Signals

AXUV Photodiode Electrical Signal

$$S_i[\mathrm{V}] = G_1\left[\frac{V}{A}\right] G_2\left[\frac{V}{V}\right] \mathcal{R}_0\left[\frac{\mathrm{A}}{\mathrm{W}}\right] \frac{\eta[\mathrm{m}^2\mathrm{sr}]}{4\pi} B_i\left[\frac{\mathrm{W}}{\mathrm{m}^2}\right]$$

L. Delgado-Aparicio, 2014

G_1 – TIA gain, G_2 – voltage amplifier gain, η – etendue of the diode channel line-of-sight (LOS)

$\boldsymbol{\mathcal{R}_0}$ – ideal diode responsivity as a **constant** value

Brightness – line-integrated plasma emissivity

$$B_i = \int \varepsilon_{\mathrm{tot}}\, dl \;\; \text{where} \;\; \varepsilon_{\mathrm{tot}} = \sum_{\mathrm{n}=0}^{12} \varepsilon_{\mathrm{Al\,n+}}$$

$\varepsilon_{\mathrm{tot}}$ – total emissivity modeled by STRAHL, dl – line-element along the channel LOS, n – aluminum charge states

LBO photodiodes are unfiltered – captures signals in the spectral range of 0.4 nm to 1100 nm

Therefore the responsivity is not constant but a function of wavelength λ, **responsivity function $\boldsymbol{\mathcal{R}_\lambda}$**.

$$B_i = \iint \varepsilon_{\mathrm{tot}}(x,\lambda)\mathcal{R}_\lambda\, dl\, d\lambda$$

Using the STRAHL Code

STRAHL (R. Dux, 2006) is a 1D transport code that solves the coupled continuity equation of all impurity charge states

$$\frac{\partial n_{I,z}}{\partial t} = \frac{1}{r}\frac{\partial}{\partial r} r \left(D \frac{\partial n_{I,z}}{\partial r} - v n_{I,z} \right) + Q_{I,z}$$

<u>STRAHL Inputs</u>

- Cylindrical plasma geometry
- ADAS (Atomic Data and Analysis Structure) database
- Experimental radial profiles of T_e, n_e, T_I and n_H
- Impurity diffusion coefficient $D = 2\ [\mathrm{m}^2/\mathrm{s}]$ and convective velocity $v = 0\ [\mathrm{m}/\mathrm{s}]$ are constant across r/a

'Typical' QHS Background Plasma Parameters

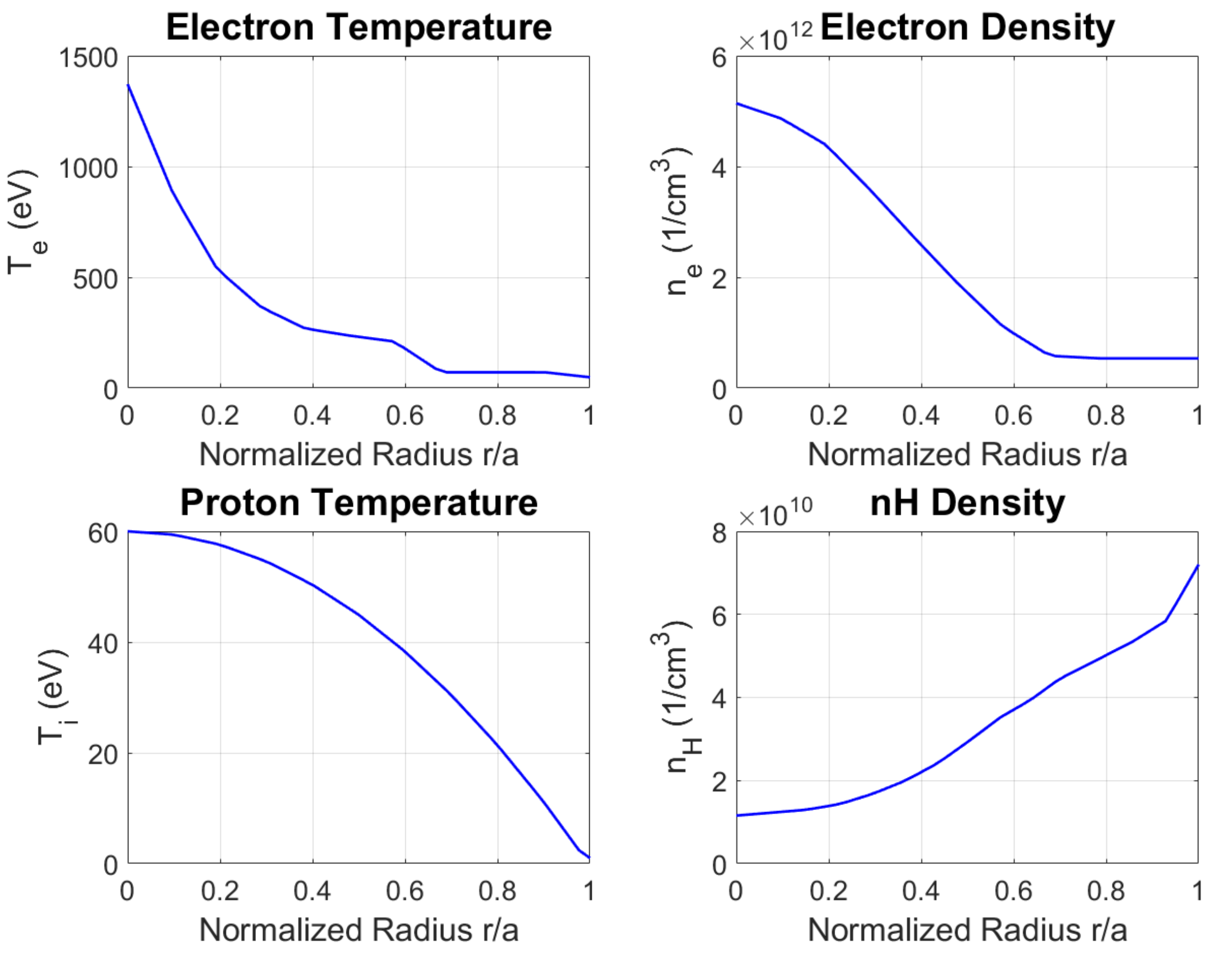

How STRAHL Results are Analyzed

STRAHL Outputs

Total Impurity Emissivity

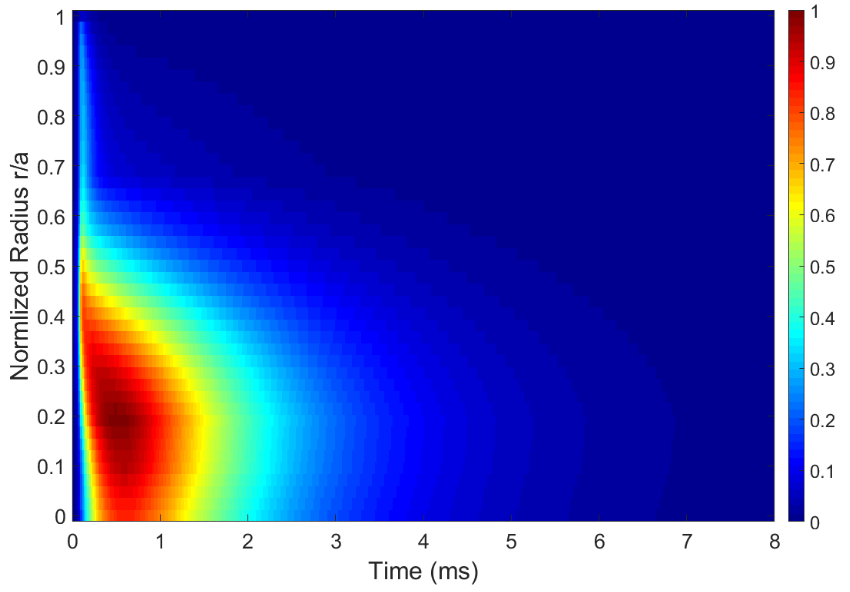

Al Charge States at **0.10 ms**

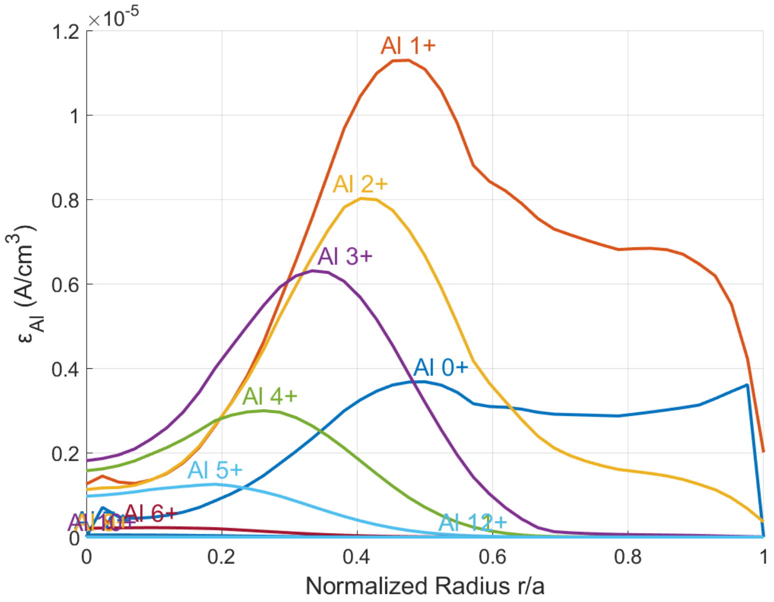

Al Charge States at **0.80 ms**

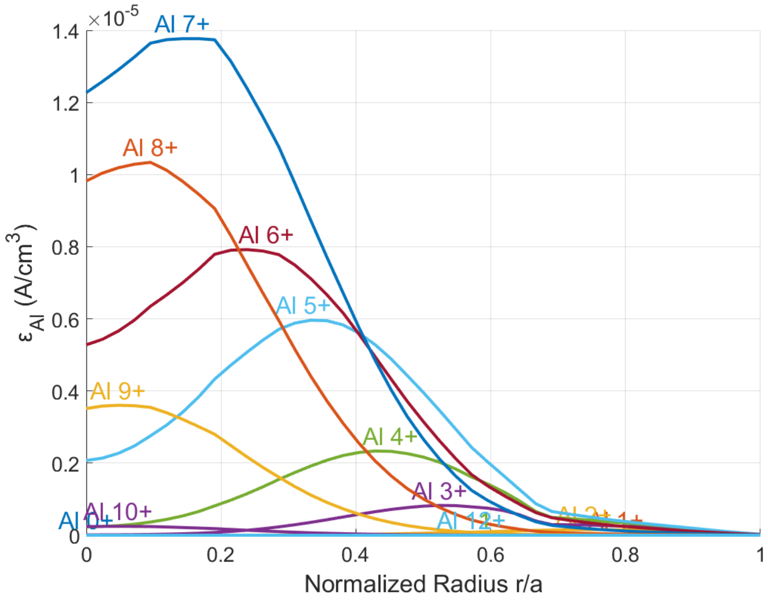

Total Emissivity refers to the sum of all aluminum charge states

- Initial intensity starts at **0.10 ms**
- After **0.80 ms**, large increase in core region

- Dominant ionization stages occur away from edge region
- Lower charge states

Al 1+, Al 2+, Al 3+

- Dominant ionization stages occur at core region
- Higher charge states

Al 6+, Al 7+, Al 8+

Impurity Confinement Time Can Be Measured after 1 ms

Log of Emissivity

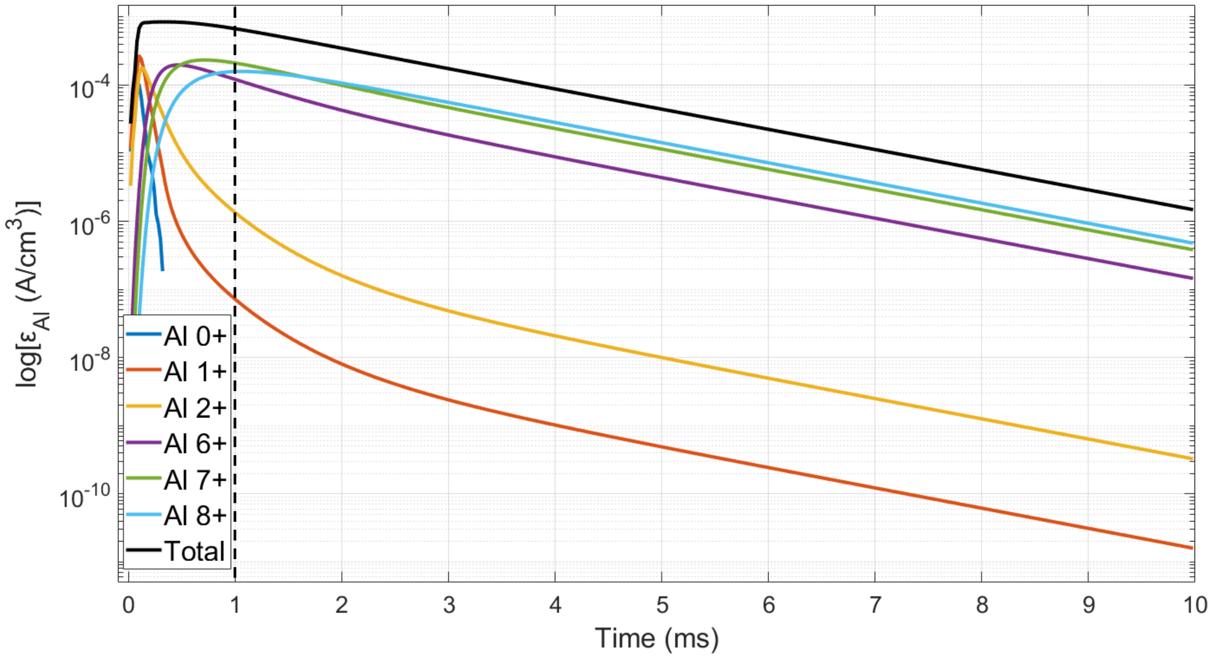

- Line-of-sight (LOS) integrated charge states of emissivity
- Black line is total sum of all LOS integrated signals: $\boldsymbol{\tau = 1.47\ \mathrm{ms}}$
- After 1 ms, slope of total emissivity is the same as highest charge states:

  Al 6+, Al 7+ and Al 8+

A common technique to deduce impurity confinement time is by measuring decay time of the highest observable charge state (R. Burhenn, 2009)

Dependence of Impurity Confinement on Power exhibit a τ~P^{-1} Scaling

Absorbed Power Scan

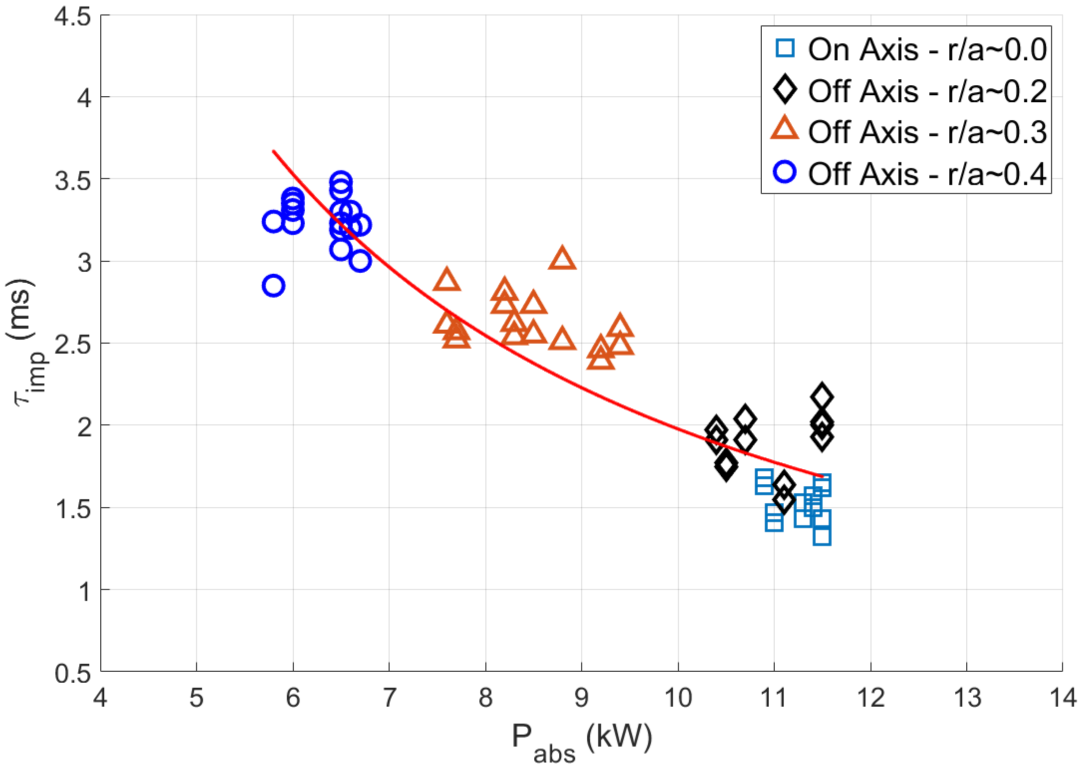

Heating location varied – off-axis heating changes power

- Exponentially fitting after 1 ms used to infer τ_{imp}

Analysis suggest $\boldsymbol{\tau_{imp}} \propto \boldsymbol{P_{\mathrm{ECRH}}}^{-1.1}$

Electron Density Scan

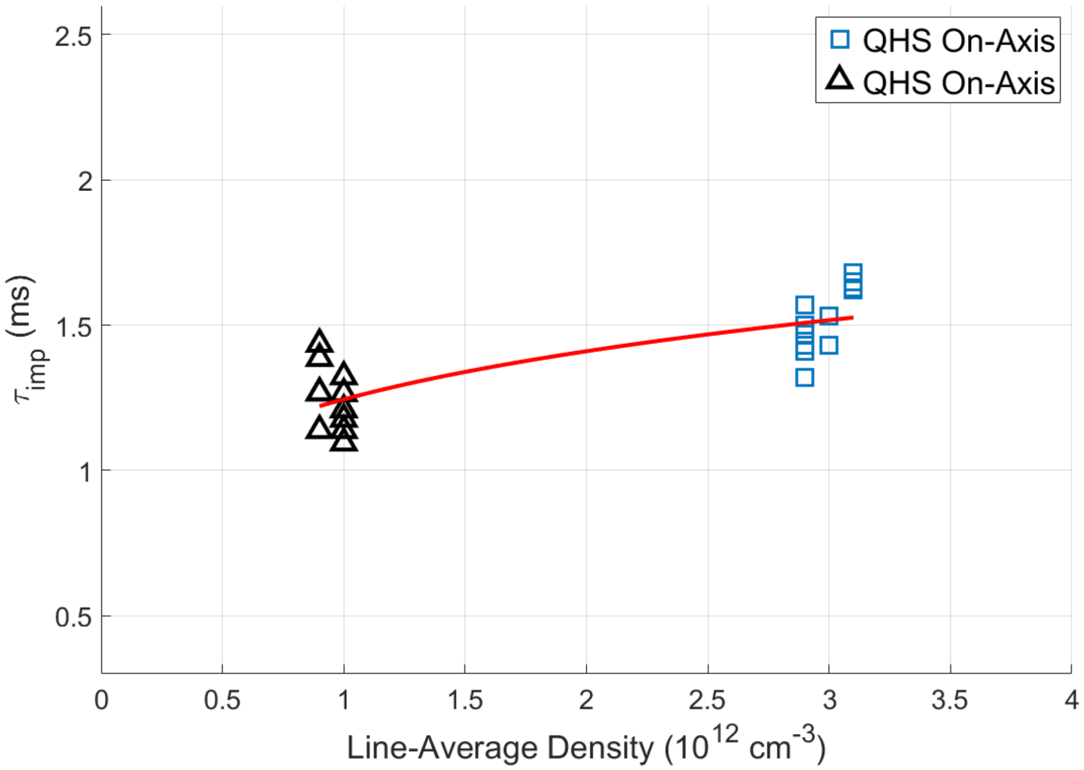

Two line-average electron densities

- $3 \times 10^{12}\ \mathrm{cm}^{-3},\ \tau_{imp} \sim 1.5\ \mathrm{ms}\ ,\ P_{abs} \sim 11.3\ \mathrm{kW}$
- $1 \times 10^{12}\ \mathrm{cm}^{-3},\ \tau_{imp} \sim 1.2\ \mathrm{ms}\ ,\ P_{abs} \sim 10.1\ \mathrm{kW}$

With only 2 data sets $\boldsymbol{\tau_{\mathrm{imp}}} \propto \boldsymbol{n_{\mathrm{e}}}^{0.2}$

PENTA Predicts Much Slower Decay than shown in Experiment

PENTA is a numerical tool that calculates the neoclassically-predicted impurity transport

PENTA Inputs

- Typical HSX background parameters

PENTA Outputs

- *D* and v profiles are used as inputs to STRAHL Code

STRAHL Outputs

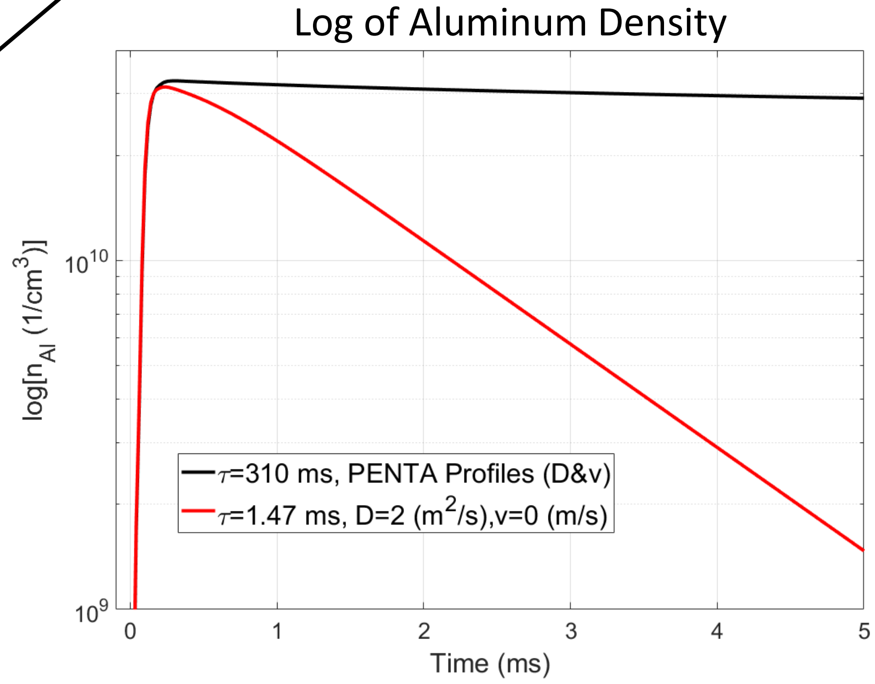

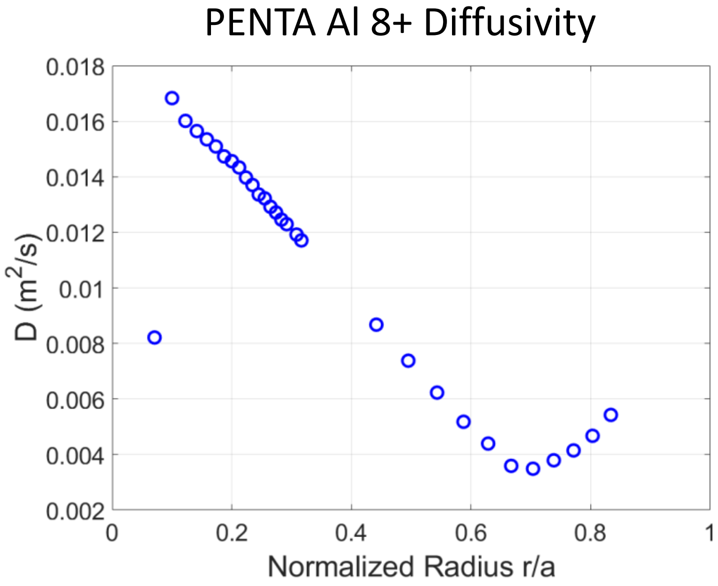

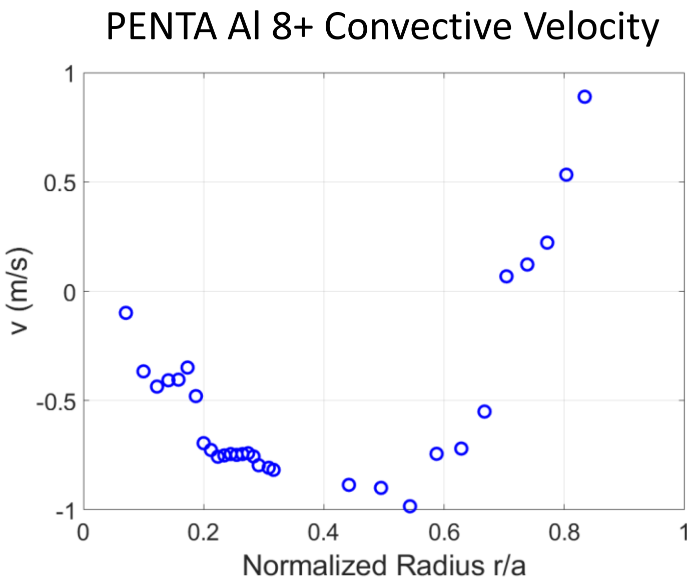

The black line represents the STRAHL result when using the PENTA profile as an input

Neoclassically-predicted decay of 310 ms is much longer than experimental decay times of ~1.5 ms

Sensitivity of Diffusivity is Much More Impactful than Velocity

Comparing Diffusion Coefficients

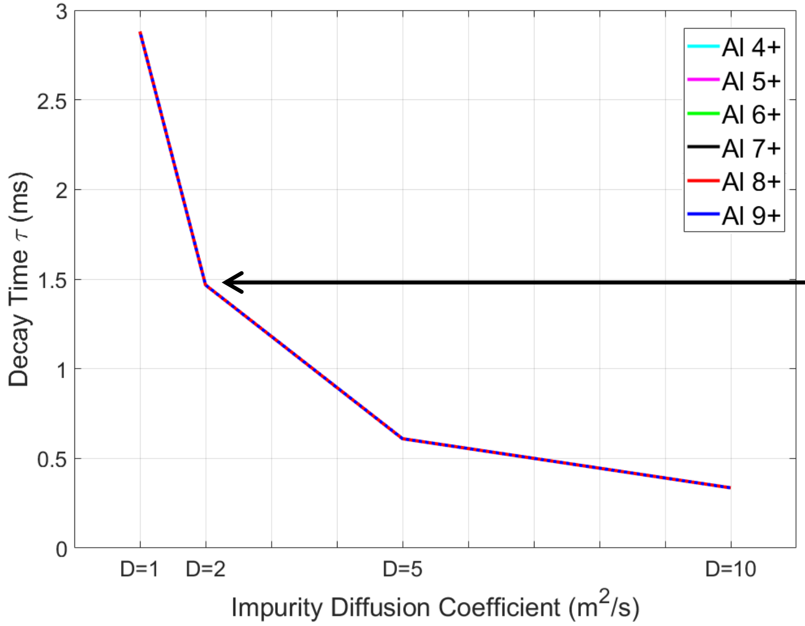

- $v = 0\ [^{\mathrm{m}}/_{\mathrm{s}}]$ is constant
- All charge states decay at the same rate

Modeled $\tau\left(D = 2\ [^{m^2}/_{s}]\right) \approx$ **1.47 ms**

is closest to experimental $\tau \approx$ **1.5 ms**

Comparing Convective Velocities

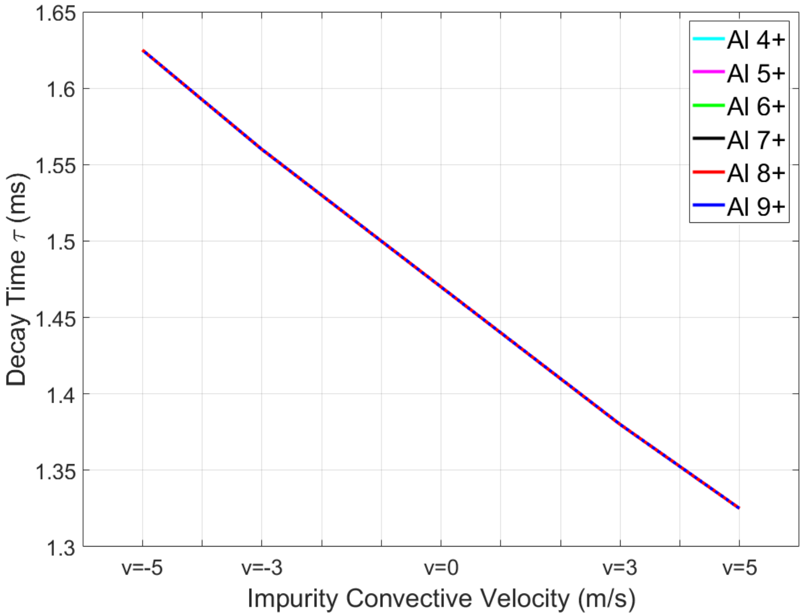

- $D = 2\ [^{\mathrm{m}^2}/_{\mathrm{s}}]$ is constant
- $\tau(v$ = -5) is only 0.3 ms larger than $\tau(v$ = +5)

Decay time shows weak linear dependence on convective velocity

Application of a Synthetic Diagnostic

Step 1: Measure each detector's sightline entry and exit points at the LCFS (last closed flux surface) with respect to the position of the chip (Cartesian coordinates).

Step 2: Discretize the vector between these 2 points into a set of Cartesian values for each channel LOS.

Step 3: Transform each Cartesian point from lab coordinates to ρ coordinates using VMEC.

Lines-of-Sight for Array A34

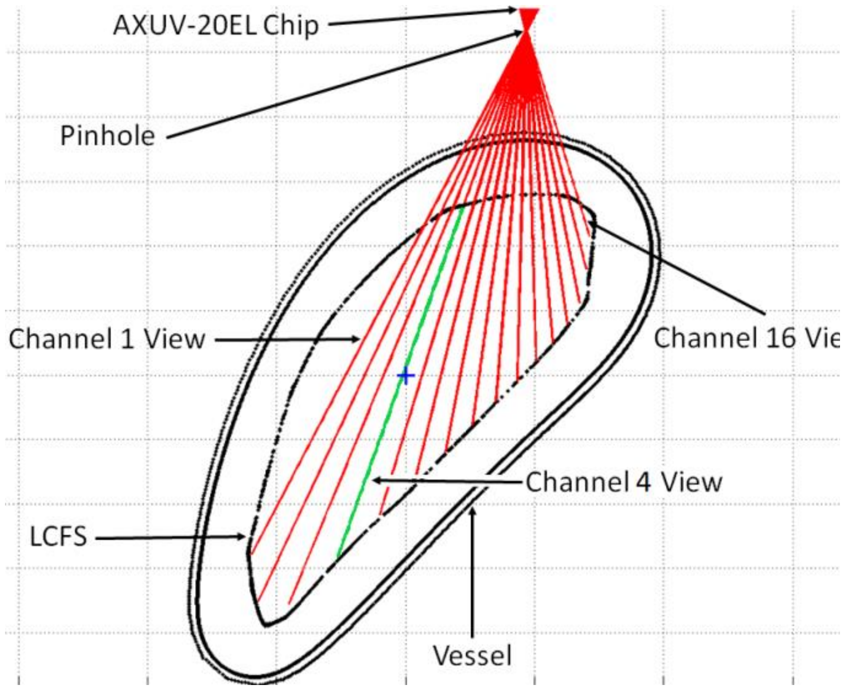

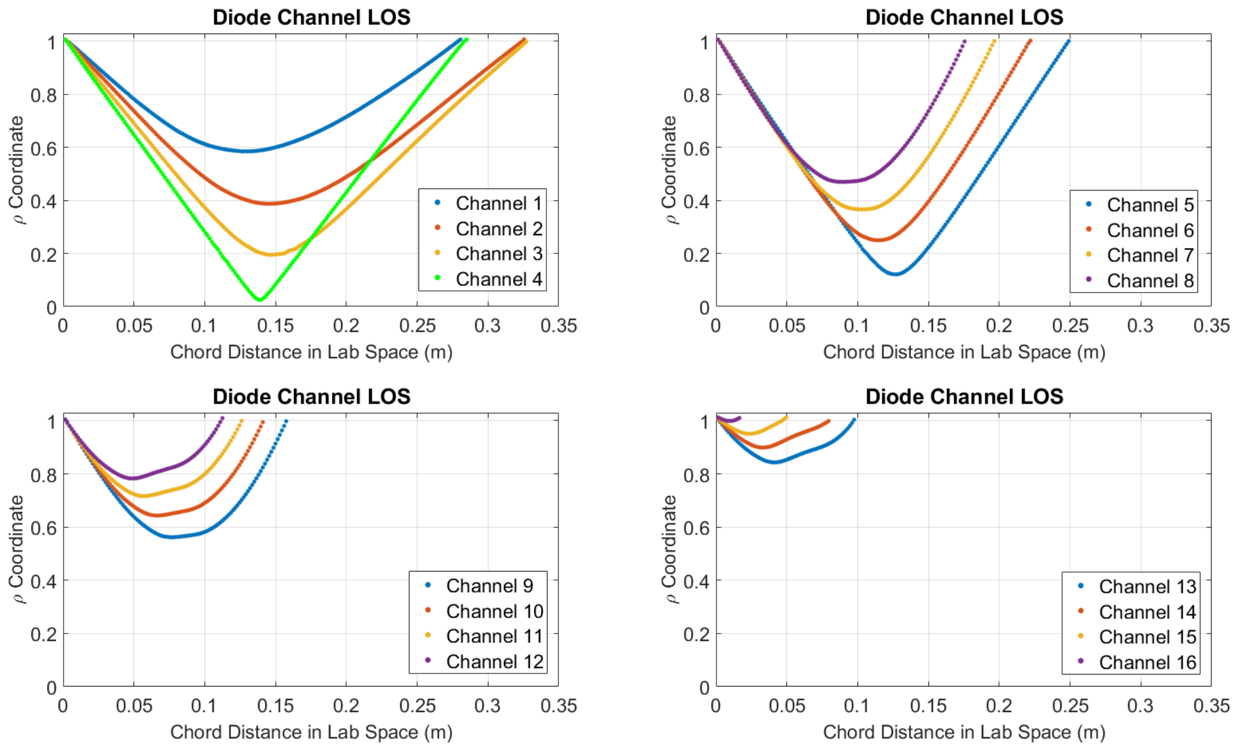

Calculated Simulated Array Signals

Step 4: The line-integrated emission, $B_i = \int \varepsilon_{\text{tot}}(x)\, dl$, for the detector LOS is interpolated from the modeled emissivity profile.

Modeled Emissivity

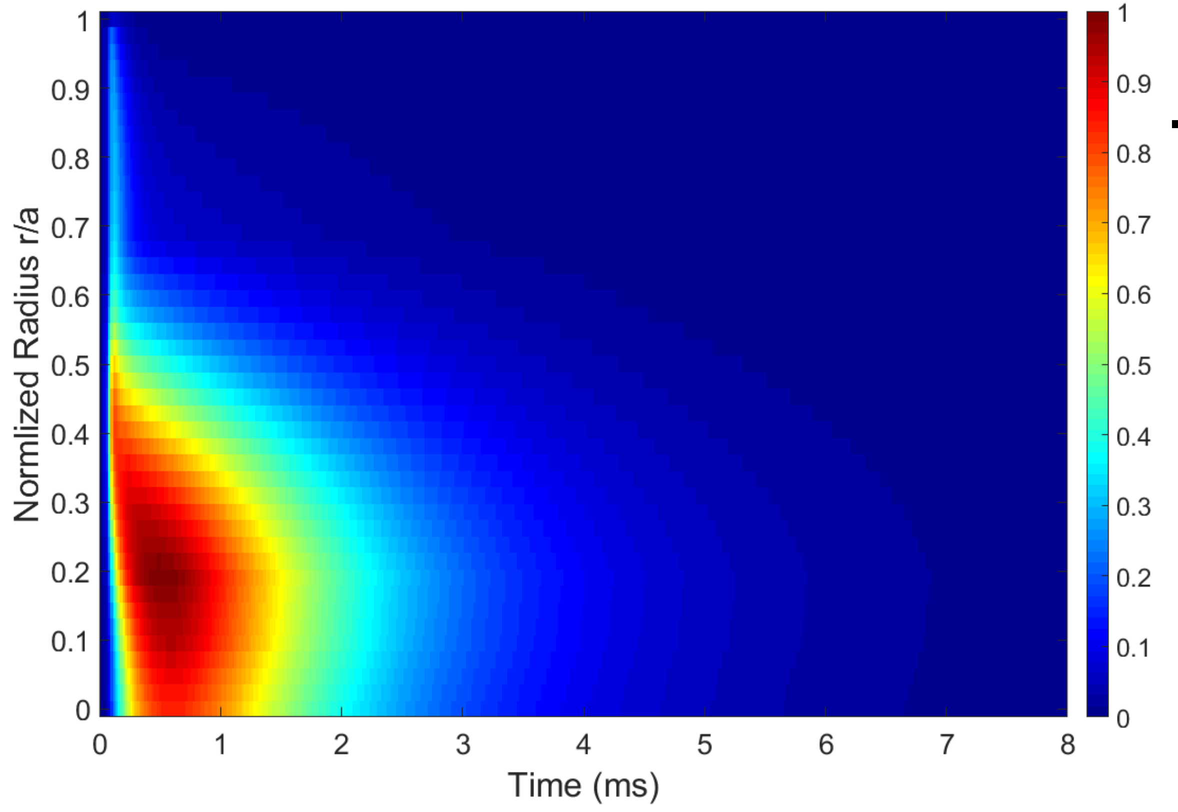

Simulated A34 Array Signal

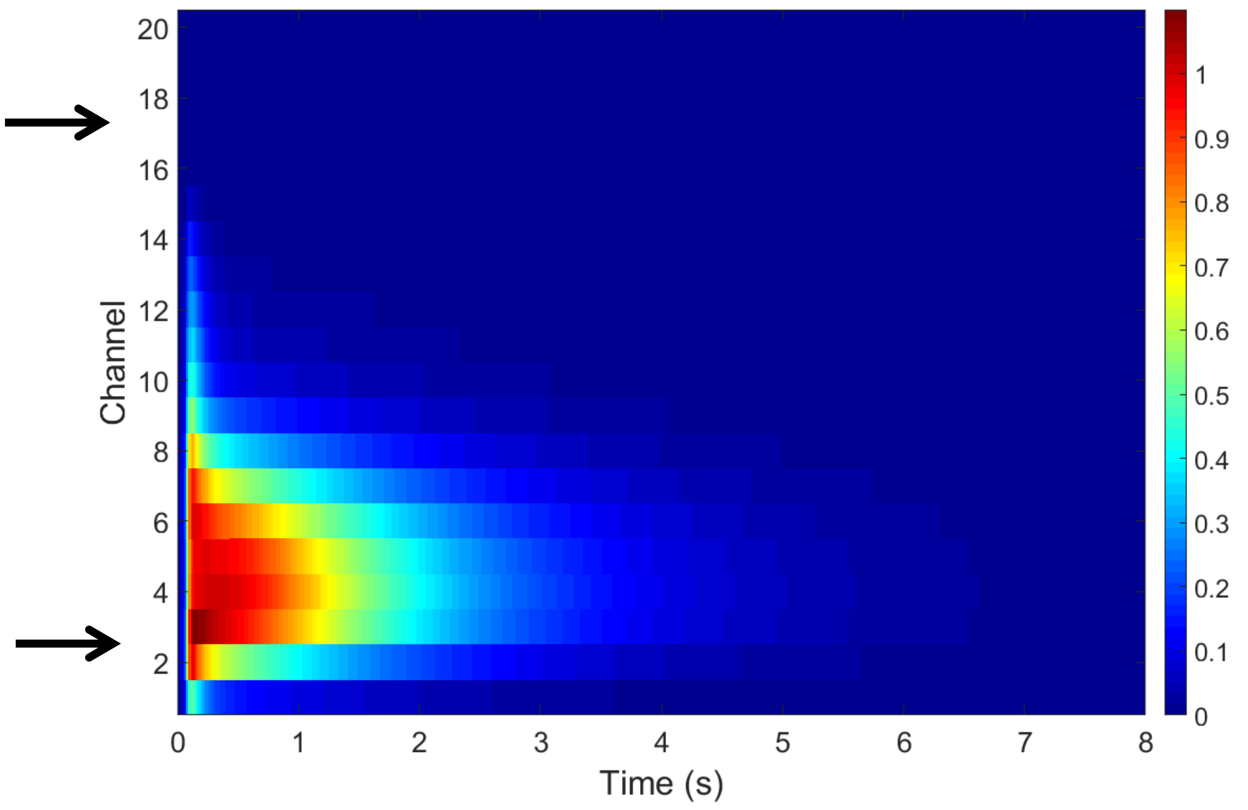

Simulated Core Signal Decay Times are Close to Experimental

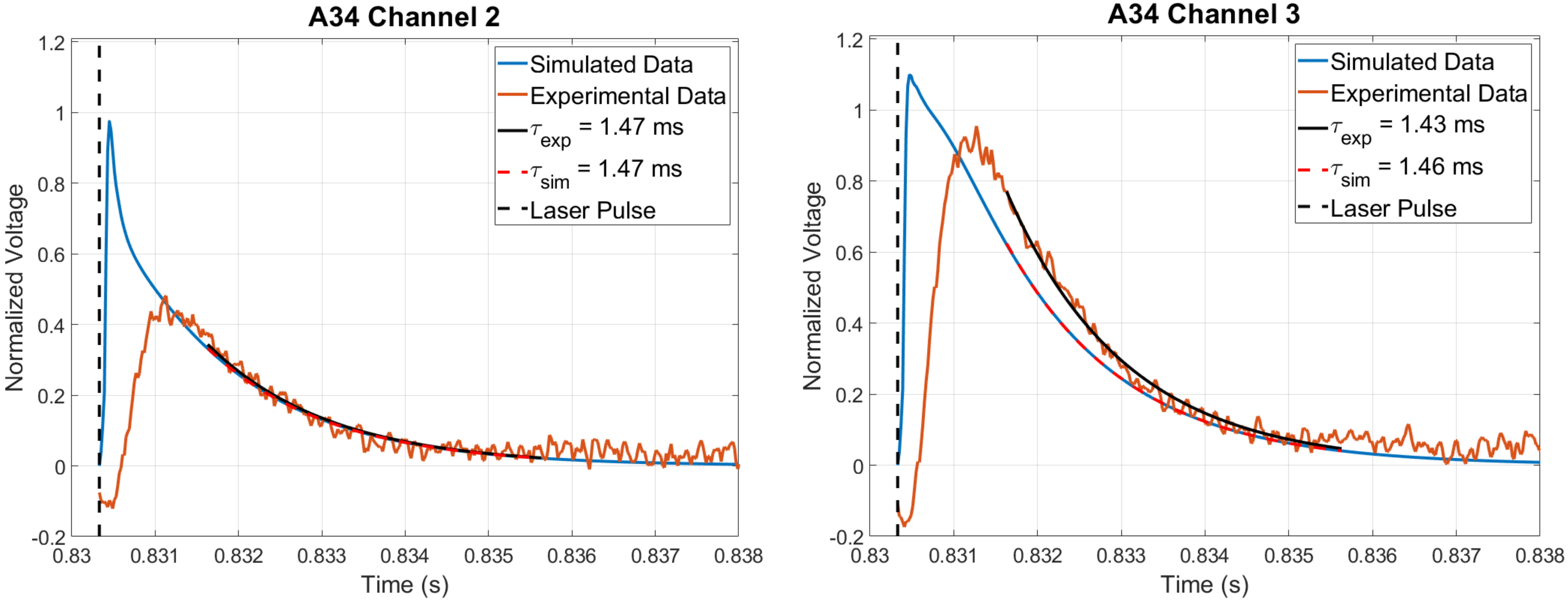

Simulated Core Signal Decay Times are Close to Experimental

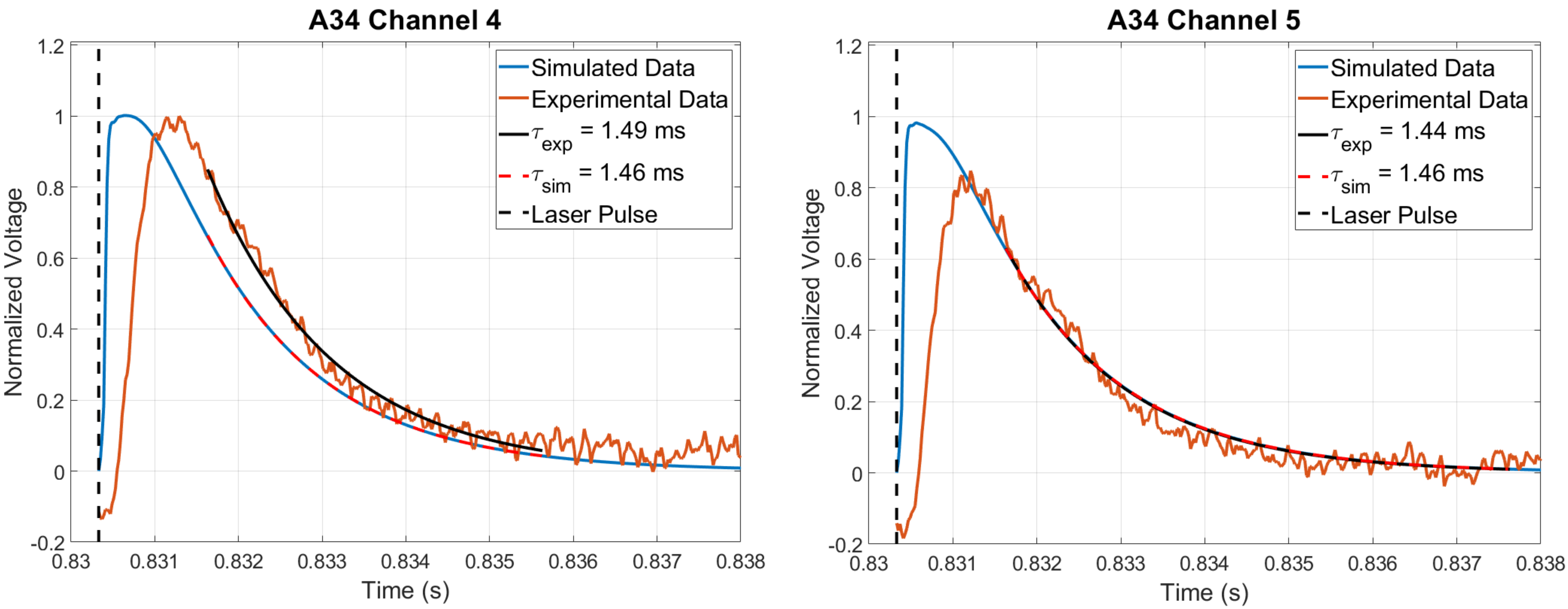

Comparing Experimental Results with Simulated Signals

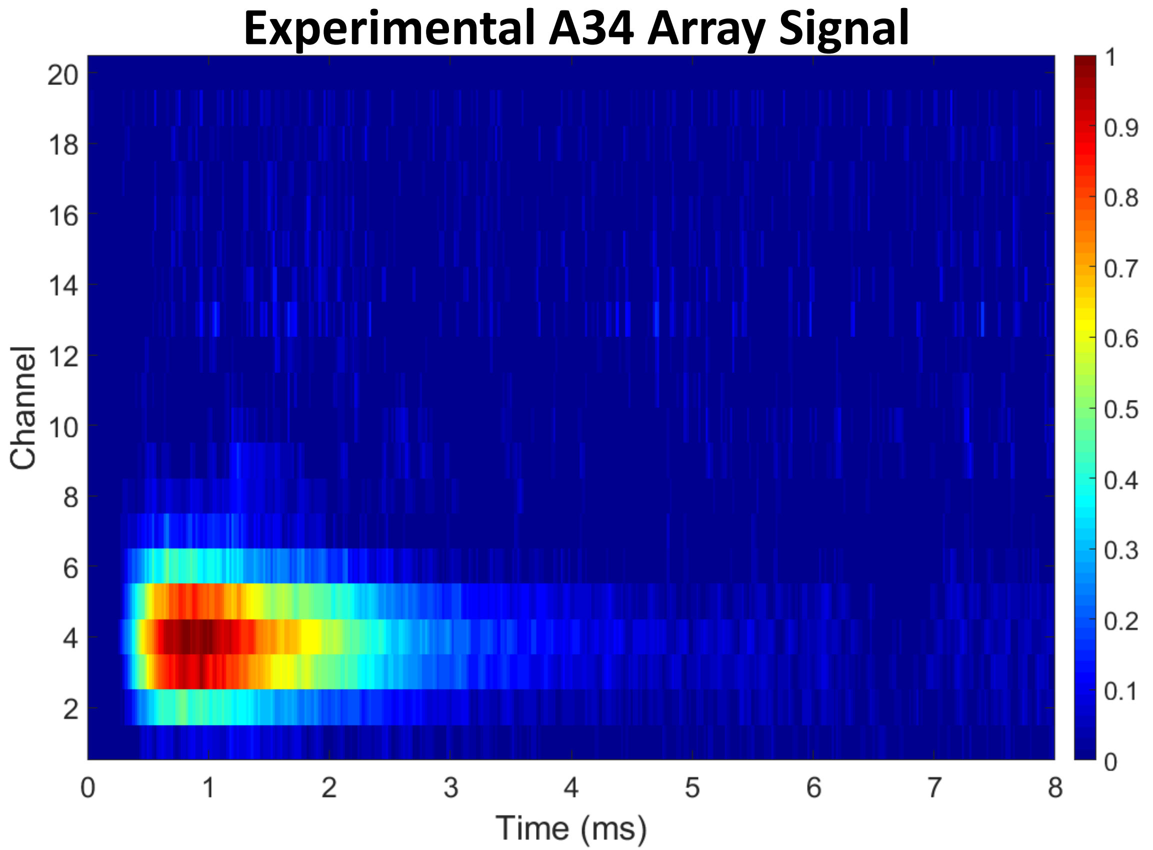

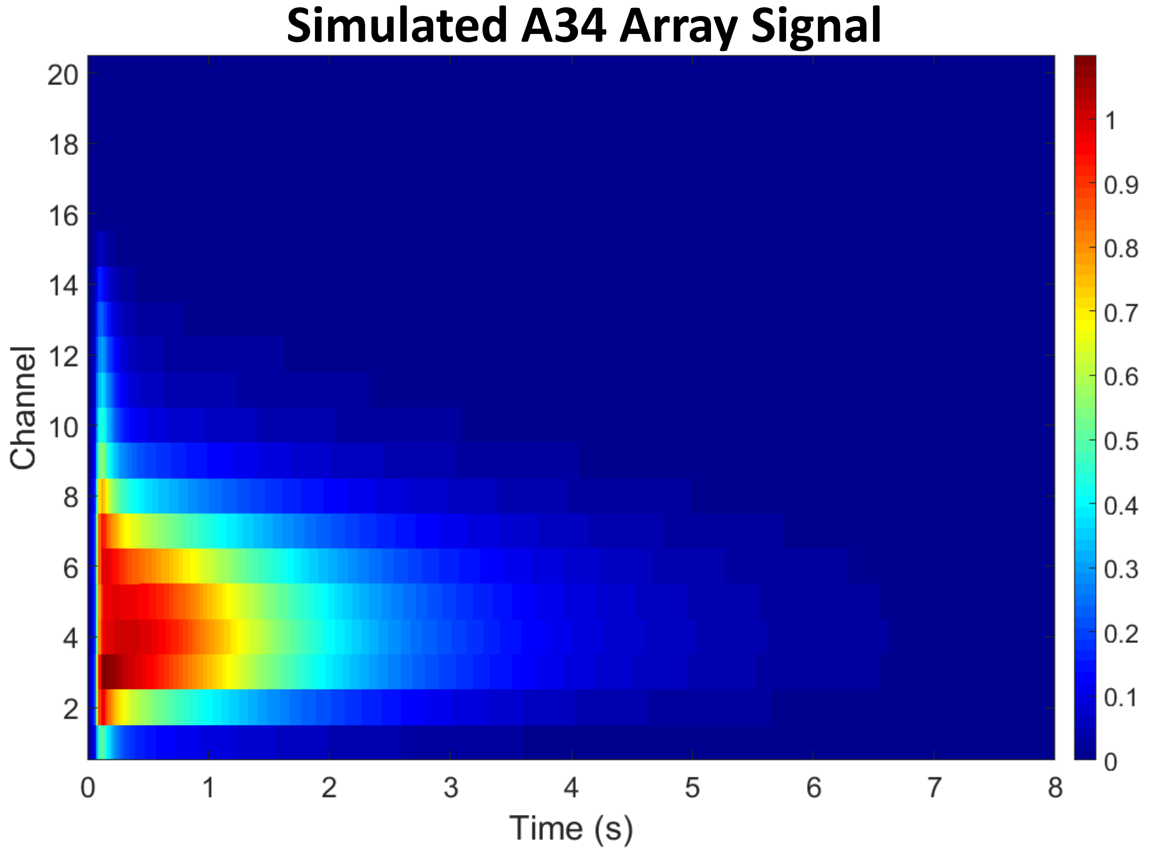

Next Step: Implement optimization algorithm with **impurity diffusivity** acting as a free parameter to minimize difference between simulated and experimental signals

$$\sum_{\text{channel}} \left(S_{\text{sim}} - S_{\text{exp}}\right)^2$$

Conclusions

- Laser blow-off experiments at HSX have produced good signal to noise measurements without strong density perturbations.
- Analysis of modeled STRAHL emissivity shows that at HSX parameters impurity confinement time can effectively be measured 1 ms after laser pulse.
- Studies of the dependence of the impurity confinement on the absorbed ECH power exhibit a $\tau \sim P^{-1}$ scaling, similar to the ISS04 scaling, suggesting a substantial impact of turbulence on the impurity confinement in HSX.
- Neoclassically-predicted calculations from the PENTA code show much longer decay times compared to experimental measurements.
- Neoclassical diffusion alone is insufficient to explain these results and suggest a substantial impact of turbulence on the impurity confinement in HSX.